Polymer 50 (2009) 5728–5732

Contents lists available at ScienceDirect

Polymer

journal homepage: www.elsevier.com/locate/polymer

Determination of polystyrene–carbon dioxide–decahydronaphthalene solution properties by high pressure dynamic light scattering

Laura Beth Dong [a], Ruben G. Carbonell [a], George W. Roberts [a,*], Douglas J. Kiserow [a,b]

[a] Department of Chemical and Biomolecular Engineering, North Carolina State University, Campus Box 7905, Raleigh, NC 27695-7905, USA
[b] U.S. Army Research Office, P.O. Box 12211, Research Triangle Park, NC 27709-2211, USA

ARTICLE INFO

Article history:
Received 15 July 2009
Received in revised form
23 September 2009
Accepted 27 September 2009
Available online 9 October 2009

Keywords:
Polystyrene
Diffusion
Dynamic light scattering

ABSTRACT

The diffusion coefficients of polystyrene (PS) in decahydronaphthalene (DHN) and in solutions of carbon dioxide (CO_2) and DHN were measured for dilute PS solutions over a range of temperatures and CO_2–DHN ratios using high pressure dynamic light scattering. Infinite dilution diffusion coefficients (D_0) of PS and dynamic second virial coefficients (k_D) were determined for essentially monodisperse 308 kDa PS. At a system pressure of 20.7 MPa, PS diffusion coefficients increased by a factor of 2.5, and the activation energy of diffusion decreased by approximately 16% when DHN was "expanded" with 44 mol% CO_2. However, the hydrodynamic radius of PS at a given temperature was not particularly sensitive to the CO_2 concentration. Solvent quality, as measured by k_D, decreased at higher CO_2 concentrations. The addition of CO_2 to polymer solutions may offer a way to "tune" the properties of the solution to facilitate the heterogeneous catalytic hydrogenation of polymers.

1. Introduction

Catalytic polymer hydrogenation can provide an efficient means to synthesize novel polymers and can offer advantages over the polymerization of the corresponding monomers [1–3]. Since catalyst residuals in the product polymer can result in product degradation and high cost, complete catalyst removal is usually required. In this case, heterogeneous (solid) catalysts are more attractive than their homogeneous counterparts because the solid catalyst is easier to recover from the polymer solution.

The kinetics of polymer hydrogenation are often hindered by mass transport limitations associated with the high viscosity of the polymer solution and the low diffusivity of the polymer molecules. These transport difficulties can be particularly troublesome in reactions catalyzed by porous solids. With porous catalysts, the unhydrogenated polymer must diffuse through the catalyst pores and adsorb to active catalytic sites in the interior of the particle. The hydrogenated polymer must then diffuse out of the particle through these pores.

Conducting heterogeneously-catalyzed polymer reactions in organic solvents expanded with carbon dioxide (CO_2) is a way to both reduce transport limitations and approach chemical processing in an environmentally-friendly manner. Carbon dioxide-expanded liquids (CXLs), a class of solvents in which CO_2 is dissolved in organic liquids, have been used as reaction media for small-molecule reactions. The amount of organic solvent required for a chemical reaction can be significantly reduced with the use of a CO_2-expanded solvent. For example, the volumes of organic solvent required for 2,6-di-*tert*-butylphenol oxidation, cyclohexene oxidation, or 1-octene hydroformylation were reduced by as much as 80% when the CO_2-expanded analogs were used [4–6].

While the addition of CO_2 to an organic solution can result in a significant decrease of solution viscosity and an increase in solute diffusion coefficient, solvent quality may also decrease as CO_2 concentration increases. Solvent quality is particularly important in polymeric systems since it affects the structure of polymer chains. Moreover, at some CO_2 concentration, the polymer chain will collapse and precipitate. Quantifying the effect of CO_2 on polymer chain dynamics will help to understand transport properties, to define the conditions that need to be maintained for polymer solubility, and may lead to a better understanding of how the polymer adsorbs to catalytic sites.

The focus of this research is the polystyrene (PS)–CO_2–decahydronaphthalene (DHN) system. Hydrogenation of the aromatic rings of PS produces polymers with improved thermal and oxidative resistance [3] and higher glass transition temperatures [7,8]. Supported nickel, palladium, and platinum catalysts have been used to saturate the aromatic rings of PS dissolved in various solvents [7,9–11], including DHN. The high boiling point of DHN relative to other solvent candidates makes it quite suitable for aromatic ring hydrogenation.

* Corresponding author. Tel.: +1 919 515 7328; fax: +1 919 515 3465.
E-mail address: groberts@eos.ncsu.edu (G.W. Roberts).

0032-3861/$ – see front matter © 2009 Elsevier Ltd. All rights reserved.
doi:10.1016/j.polymer.2009.09.069

Moreover, DHN can dissolve approximately 60 mol % CO_2 before PS precipitation occurs [12]. Finally, the hydrogenation rate of PS in CO_2-expanded DHN was shown to be one and a half times faster than the same reaction in DHN [12].

While these outcomes are favorable, the behavior of PS in CO_2-expanded DHN is not well understood. A more complete understanding of this behavior should lead to the design of improved catalysts and allow reaction conditions to be tuned for high reaction rates and selectivities. In this research, high pressure dynamic light scattering (DLS) was used to measure the effect of CO_2 on the PS diffusion coefficient in DHN. The effects of CO_2 concentration on solvent quality and PS hydrodynamic radii were also quantified.

Dynamic light scattering has been used to probe polymer solution properties for over 40 years. The use of high pressure DLS to understand polymer-supercritical fluid solution properties emerged in the late 1990s. Kermis et al. used high pressure DLS to measure poly(ethylene-co-1-butene) diffusion in various alkanes under supercritical conditions [13]. More recently, the high pressure technique has been used to study CO_2–poly(dimethylsiloxane) (PDMS) [14] and CO_2-fluorinated alkyl methacrylate [15] systems. The solvating power of CO_2 was found to be dependent on CO_2 density for both systems. The hydrodynamic radius of PDMS did not vary significantly with increasing CO_2 density. However, the hydrodynamic radius of the fluorinated alkyl methacrylate increased about 10% with CO_2 density increasing from 0.85 to 1.05 g/mL. The present research on the PS–CO_2–DHN system is the first known use of high pressure DLS to study solutions of a polymer dissolved in a CO_2-expanded liquid.

2. Experimental

2.1. Materials

Essentially monodisperse PS was purchased from Polymer Source, Incorporated (Montreal, Canada) and used as received. The number-average molecular weight (M_n) was 308 kDa, and the polydispersity index (PDI) was 1.04, both determined by gel permeation chromatography (GPC). The corresponding values reported by the supplier were 412 kDa and 1.05. Anhydrous DHN (24% *cis*, 76% *trans*) was purchased from Sigma Aldrich (St. Louis, MO). Carbon dioxide (≥99.99%) was purchased from National Welders (Charlotte, NC).

2.2. Polystyrene solution preparation

DHN was filtered through a 0.2 μm Millex polytetrafluoroethylene (PTFE) syringe filter (Millipore Corporation, Billerica, MA) before it was used to dissolve PS. The polymer solution was filtered through a 5 μm Millex PTFE syringe filter (Millipore, Corporation, Billerica, MA) before it was loaded into the DLS cell.

2.3. Molecular weight measurement

Gel permeation chromatography was used to measure the molecular weight of polystyrene. A Waters Alliance GPC system (Waters Corporation, Milford, MA) equipped with Styragel HR3, HR4, and HR4E columns (Waters Corporation, Milford, MA) was used. A miniDAWN Tristar light scattering detector (Wyatt Technology, Santa Barbara, CA) in combination with a refractive index detector (Optilab® rEX, Wyatt Technology, Santa Barbara, CA) were used to measure polymer molecular weight and polydispersity index. Tetrahydrofuran (HPLC grade, Fisher Scientific, Pittsburgh, PA) was the mobile phase.

A Waters 150-CV GPC system (Waters Corporation, Milford, MA) equipped with Styragel HR5, HR4, HR2, and HR 0.5 columns (Waters Corporation, Milford, MA) and a refractive index detector was used to confirm the results provided by the Alliance system. The mobile phase was THF (Fisher Scientific, Pittsburgh, PA), and polystyrene standards were used for calibration. The averages of M_n and PDI obtained from three independent measurements on the two GPC systems are reported. The averaged M_n values ranged from 301 to 312 kDa while PDI values were between 1.03 and 1.04.

2.4. Dynamic light scattering

A 532 nm-solid state laser (Crystalaser, Reno, NV) was used as the light source. The high pressure DLS sample cell was custom-built. Scattered light intensities were measured at 90° from the light source. The cell temperature was maintained by circulating silicone fluid through a custom-made heating jacket.

For the diffusion coefficient measurements in CO_2-expanded DHN, a known amount of CO_2 was loaded into the cell via one of two methods. For the lowest CO_2 concentration, the amount of delivered CO_2 was determined gravimetrically. For the higher CO_2 concentrations, a known volume of CO_2 was delivered by an ISCO syringe pump (Teledyne ISCO, Lincoln, NE). A manual high pressure generator (High Pressure Equipment Company, Erie, PA) was used to pressurize the system to 20.7 MPa. At all of the experimental temperatures, the CO_2-containing solutions are in a single liquid phase at this pressure.

A photomultiplier tube and TurboCorr digital autocorrelator card (both Brookhaven Instruments, Holtsville, NY) were used to measure the normalized, intensity–intensity correlation function, $g_2(t)$. The scattered intensity is related to the electric field autocorrelation function, $g_1(t)$, through Equation (1).

$$g_2(t) = B\left(1 + \beta|g_1(t)|^2\right) \tag{1}$$

In Equation (1), B is the measured baseline and β accounts for non-ideal factors such as the area of the detector. For monodisperse, dilute polymer solutions, the electric field autocorrelation function is exponentially dependent on the characteristic decay rate, Γ, through Equation (2).

$$g_1(t) = \exp(-\Gamma t) \tag{2}$$

Combining Equations (1) and (2),

$$g_2(t) = B\left(1 + \beta|\exp(-\Gamma t)|^2\right) \tag{3}$$

The characteristic decay rate is a function of the translational diffusion coefficient, D, and the square of the scattering vector, q, as shown in Equation (4).

$$\Gamma = \mathrm{q}^2 D \tag{4}$$

The scattering vector is a function of the scattering angle (θ), the solvent's refractive index (n_{mix}), and the incident wavelength of light (λ), as shown below.

$$\mathrm{q} = \frac{4\pi n_{mix}}{\lambda}\sin\left(\frac{\theta}{2}\right) \tag{5}$$

The Lorenz–Lorentz equation was used to calculate the refractive indices of the CO_2-expanded DHN mixtures. As shown in Equation (6), the refractive index of the mixture (n_{mix}) is dependent on the mass fractions of the components (w_i), the component refractive indices (n_i), the component densities (ρ_i), and the mixture density (ρ_{mix}).

$$\frac{n_{mix}^2 - 1}{n_{mix}^2 + 2} = \rho_{mix}\left[\frac{w_1}{\rho_1}\frac{n_1^2 - 1}{n_1^2 + 2} + \frac{w_2}{\rho_2}\frac{n_2^2 - 1}{n_2^2 + 2}\right] \tag{6}$$

In order to use the Lorenz–Lorentz equation, Hammel et al.'s

refractive index data for DHN [16] and Michels et al.'s CO_2 data [17] were extrapolated. The densities of CO_2 were calculated from the NIST Thermophysical Properties database [18] and DHN densities were determined from the DIPPR database [19]. The densities of the CO_2–DHN mixtures were obtained from Cain [20]. The calculated values of n_{mix} were used to calculate values of q for each experiment using Equation (5).

The diffusion coefficients of PS (D) were obtained by minimizing the sum of the squares of the deviations between the measured values of $g_2(t)$ and Equation (3), to find the "best" values of Γ, B, and β. Once q was calculated from Equation (5), Equation (4) was used to calculate D.

In the dilute solution regime, the measured diffusion coefficients of PS should exhibit a linear dependence on polymer concentration (C) as shown in Equation (7), where D_0 is the infinite dilution diffusion coefficient and k_D is the dynamic second virial coefficient:

$$D = D_0(1 + k_D C) \tag{7}$$

The infinite dilution diffusion coefficient can be used to calculate the hydrodynamic radius (R_H) of the dissolved polymer via the Stokes–Einstein equation, Equation (8).

$$R_H = \frac{k_B T}{6\pi\eta D_0} \tag{8}$$

Here, k_B is the Boltzmann constant, and T is the absolute temperature. Viscosities (η) for the *cis*/*trans*-DHN mixture were interpolated from data by Cain [20], while CO_2–DHN viscosities at 20.7 MPa were measured by Cain [20]. Since the form factor, i.e., the product of q and R_g (the radius of gyration of the polymer coil), was less than one for all experiments, the angular dependence of D should be weak and was neglected. Values of R_g were estimated as $R_H\sqrt{3/5}$.

3. Results and discussion

3.1. PS diffusion in pure DHN

As shown in Fig. 1, the diffusion coefficients of PS in DHN were found to be linearly dependent on polymer concentration between 0.111 and 0.50 wt% PS, for temperatures ranging from 297 K to 392 K. The infinite dilution diffusion coefficients were determined by extrapolating to zero polymer concentration. The dynamic second virial coefficients were calculated from the slopes of the straight lines and the D_0's. These two values, along with the hydrodynamic radii calculated from Equation (8), are provided in Table 1.

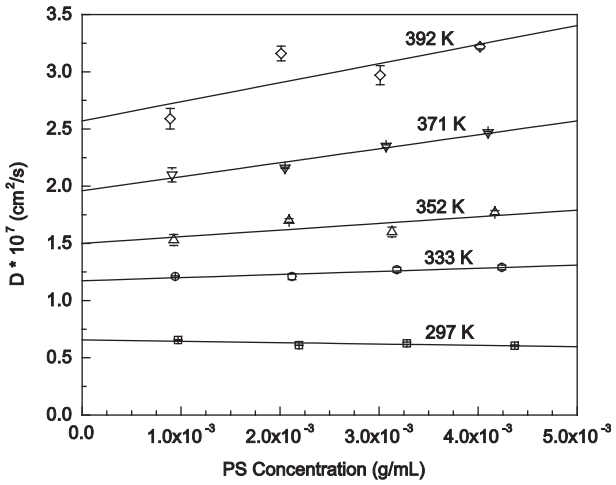

Fig. 1. Dependence of PS diffusion coefficients on PS concentration and temperature (PS $M_n = 308$ kDa, PDI = 1.04). The error bars represent the standard deviations of three diffusion coefficient measurements.

Table 1
PS Diffusion in DHN.

T (K)	$D_0 \times 10^7$ (cm^2/s)	k_D (mL/g)	R_H (nm)
297	0.656	−18.0	14.2 ± 0.6
333	1.17	23.3	16.4 ± 0.7
352	1.50	38.7	17.7 ± 1.7
371	1.96	62.2	17.8 ± 1.1
392	2.57	65.0	18.0 ± 2.6

PS $M_n = 308$ kDa, PDI = 1.04. The errors for R_H were calculated as described in the Supporting information.

Infinite dilution diffusion coefficients increased roughly four-fold as temperature was increased from 297 K to 392 K. The D_0's at 333 K and 352 K were compared to Kotera et al.'s data for a 450 kDa PS in *trans*-DHN. These investigators used a modified electrophoretic apparatus to measure diffusion coefficients. The values obtained in this research (1.17×10^{-7} and 1.50×10^{-7} cm^2/s, respectively) are in good agreement with the previously reported values (1.1×10^{-7} and 1.45×10^{-7} cm^2/s) [21]. When the present results are scaled to a molecular weight of 450 kDa using $D \propto (\text{molecular weight})^{-0.5}$, the comparison becomes 0.968×10^{-7} and 1.24×10^{-7} cm^2/s, respectively.

The dynamic second virial coefficient, an indicator of solvent quality, is related to the osmotic second virial coefficient (A_2), the polymer molecular weight (M), the first order friction coefficient (k_F), and the polymer specific molar volume (ν_2) as shown in Equation (9) [22].

$$k_D = 2A_2M - k_F - \nu_2 \tag{9}$$

Tsunashima and co-workers reported negative k_D values at a theta temperature of 293.4 K for a series of high molecular weight PS's dissolved in *trans*-DHN [23]. These negative k_D values are reasonable since $A_2 = 0$ at the theta temperature of a polymer-solvent system. The negative k_D at 297 K that was obtained in this research is consistent with this analysis and the data of Tsunashima et al.

At temperatures greater than the theta temperature, A_2 is positive, and it increases as solvent quality improves [24], e.g. k_D values are expected to become more positive as the temperature increases. The k_D values reported in Table 1 are consistent with the normal behavior of A_2, as k_D transitions from negative to increasingly positive values over the temperature range studied.

The increase in R_H with temperature shown in Table 1 indicates that the PS coil relaxes as the solvent quality of DHN changes from a borderline theta condition at 297 K to the good solvent regime at higher temperatures. However, the change in R_H is not statistically significant once the solvent quality is relatively high, i.e., above about 350 K. In the good solvent regime, the observed increases in the PS infinite dilution diffusion coefficients with temperature are almost exactly compensated by decreases in viscosity.

Nose and Chu measured R_H for a monodisperse, 179 kDa (M_w) PS in *trans*-DHN at 293 K [25]. If their value (9.11 nm) is scaled to the PS molecular weight used in this research ($M_w = 320$ kDa) using the relationship $R_H \propto \sqrt{\text{molecular weight}}$, the result is 12.7 nm. This value falls slightly below the R_H obtained at 297 K in this study (14.2 nm). Since this research was conducted above the θ-temperature of PS in *trans*-DHN, Nose and Chu's R_H was also scaled with $(\text{molecular weight})^{0.6}$. The R_H marginally increased to 12.9 nm.

A slight difference in R_H can be expected since the present research used a 24% *cis*:76% *trans* mixture of DHN as the solvent for PS. Other researchers have shown that the theta temperature of a PS–DHN solution is dependent on the *cis*/*trans* ratio [26,27]. Since

the *cis* isomer is a better solvent for PS than the *trans* isomer, PS should be more relaxed, i.e., it should be larger in size, in a mixture of DHN isomers than in *trans*-DHN.

3.2. PS diffusion in CO_2-expanded DHN

The presence of CO_2 in polymer solutions is known to induce changes in solvent quality, polymer coil size, and solution viscosity [28,29]. The impact of CO_2 on PS diffusion coefficient, hydrodynamic radius, and solvent quality was determined over the same range of PS concentrations studied in the first part of this research. Previous research on the phase behavior of a moderately-concentrated PS–CO_2–DHN solution indicated that PS precipitates at a CO_2 mole fraction of approximately 60% for temperatures ranging from 313 K to 423 K [12]. In order to avoid PS precipitation, CO_2 concentrations of 14, 26, and 44 mol% were used in this research. System pressure was maintained at 20.7 MPa to ensure a single liquid phase at each experimental temperature. No PS diffusion coefficient measurements were made with CO_2-expanded DHN at 297 K and 20.7 MPa because there is evidence that CO_2 and DHN form a biphasic liquid mixture at this temperature and pressure [30].

3.2.1. PS diffusion coefficients in CO_2–DHN

The addition of almost 60 mol% CO_2 to a moderately-concentrated PS–DHN solution can reduce polymer solution viscosity by nearly two orders of magnitude [31]. Such reductions in solution viscosity should increase PS diffusion coefficients in CO_2-expanded DHN.

The D_0's for the CO_2-containing polymer solutions were obtained in the manner described in Section 3.1. The effects of temperature and CO_2 concentration on D_0 are shown in Fig. 2. At each temperature, the infinite dilution diffusion coefficients of PS increased with CO_2 concentration. In fact, D_0 increased by roughly a factor of 2.5 when the polymer solutions were expanded with 44 mol% CO_2.

The activation energies of diffusion (E) at each CO_2 concentration were calculated from the plots of the natural logarithm of the infinite dilution diffusion coefficient versus inverse absolute temperature. The values in Table 2 show that E decreases by roughly 16% as CO_2 concentration increases from 0 to 44 mol%. The decrease in E with increasing CO_2 concentration is reasonable since CO_2 reduces polymer solution viscosity and therefore the drag forces on the polymer coils.

Table 2
Effect of CO_2 concentration on the activation energy of PS diffusion.

CO_2 concentration (mol%)	E (kJ/mol)
0	12.7 ± 0.9
14	13.8 ± 0.5
26	11.1 ± 0.5
44	10.7 ± 1.0

20.7 MPa (PS M_n = 308 kDa, PDI = 1.04) The errors were defined as the standard errors of the slope in the ln (D_0) v. 1/T plots.

3.2.2. Solvent quality and PS coil size

Dynamic second virial coefficients, calculated by the method described in Section 3.1, are shown as a function of temperature and CO_2 concentration in Fig. 3. Errors for these measurements are provided in the Supporting information. The addition of 14 mol% CO_2 to PS–DHN appears to improve the solvent quality at temperatures of 372 K and lower since the k_D values for DHN containing 14 mol% CO_2 are larger than the k_D's for PS-neat DHN. At the highest temperature, the k_D for 14 mol% CO_2 in DHN is lower than that for neat DHN. However, the difference is not statistically significant. The addition of more CO_2 (beyond 14 mol%) decreases solvent quality, as indicated by k_D values that are below those of DHN–14 mol% CO_2.

The increase of solvent quality that was observed when low concentrations of CO_2 were added to DHN at low temperatures has little or no precedent in the literature. It is generally believed that adding any amount of CO_2 to an organic liquid reduces solvent quality. The optimum k_D with CO_2 concentration that was observed in this study may be specific to the CO_2–DHN system.

Li and co-workers used small-angle X-ray scatterings (SAXS) to monitor changes in solvent quality and radii of gyration of PS in CO_2–tetrahydrofuran (THF) and CO_2–toluene mixtures at 308.15 K [28,32]. The osmotic second virial coefficient (A_2) changed from positive to negative and decreased monotonically as CO_2 pressure increased from 0 to 2.7 MPa in PS (78 kDa)–THF. The change of sign for A_2 is indicative of decreasing solvent quality. Concurrently, the radius of gyration decreased from 14.0 nm to 10.5 nm [28].

The same 78 kDa PS dissolved in toluene exhibited similar behavior when CO_2 was added. The radius of gyration decreased from 9.55 to 7.13 nm as CO_2 pressure was increased from 0 to 4.2 MPa. Li et al. indicate that the latter pressure corresponds to approximately 40 mol% CO_2 dissolved in toluene. Over the same

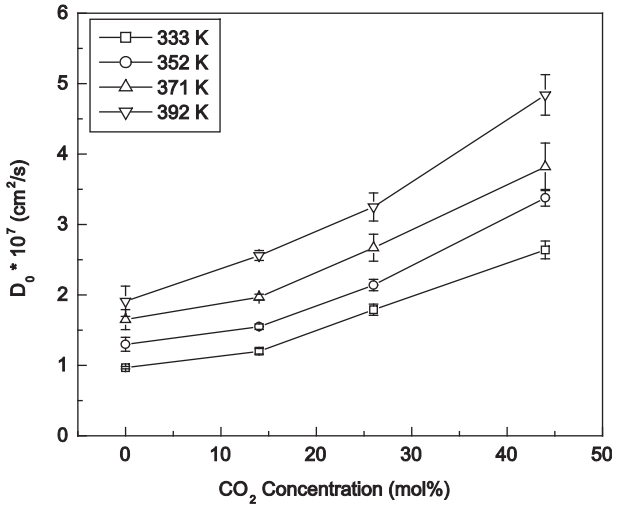

Fig. 2. Effect of CO_2 and temperature on PS infinite dilution diffusion coefficients at 20.7 MPa (PS M_n = 308 kDa, PDI = 1.04). The error bars represent the standard errors of the intercepts of the diffusion coefficient versus PS concentration plots.

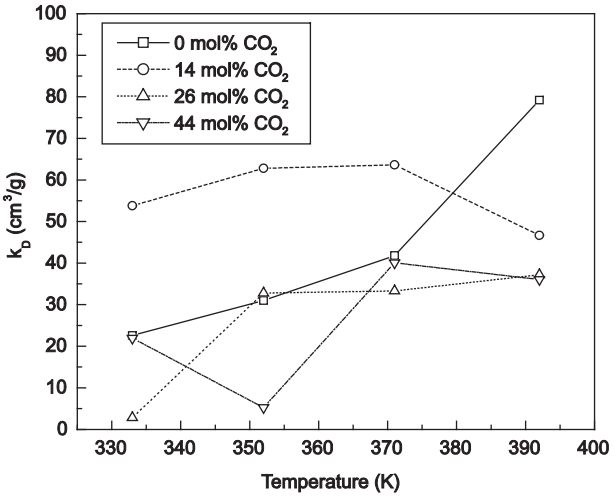

Fig. 3. Effect of temperature and CO_2 concentration on dynamic second virial coefficient at 20.7 MPa (PS M_n = 308 kDa, PDI = 1.04).

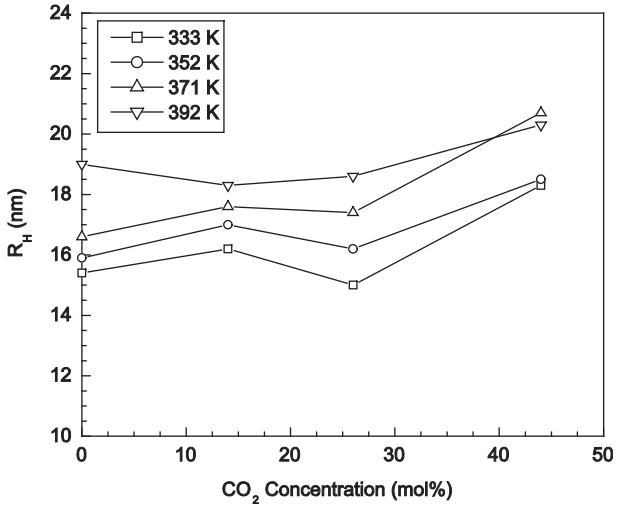

Fig. 4. Effect of CO_2 and temperature on PS hydrodynamic radii at 20.7 MPa (PS $M_n = 308$ kDa, PDI = 1.04).

CO_2 concentration range, a 40% decrease in the second virial coefficient, A_2, was observed; this is indicative of the anti-solvent power of CO_2 [32].

Fig. 4 shows the effect of CO_2 concentration on the hydrodynamic radii of PS in DHN at several temperatures. When the errors of these measurements are considered, the R_H for PS in CO_2-expanded DHN remains essentially constant as CO_2 concentration increases at each of the four temperatures. The errors in R_H are provided in the Supporting information.

These results contrast with the SAXS results in which the R_g of PS in THF or toluene decreased with increasing CO_2 concentration. The manner in which R_g and R_H are obtained differs. In SAXS, static polymer properties such as A_2 and R_g can be obtained directly from scattering data. However, with DLS, R_H must be calculated from values of D_0 and η, which are subject to some error. Finally the present experiments were conducted at constant hydrostatic pressure, whereas the hydrostatic pressure increased with CO_2 pressure in the studies of Li and co-workers [28,32].

4. Conclusions

Polystyrene diffusion coefficients in DHN and CO_2-expanded DHN were measured using high pressure dynamic light scattering between 333 and 392 K. At each temperature, the infinite dilution diffusion coefficient of PS increased as the concentration of CO_2 in DHN increased. At 44 mol% CO_2/56 mol% DHN, the diffusion coefficients were about 2.5 times greater than in pure DHN, over the range of temperatures studied. A small (14 mol%) addition of CO_2 resulted in a slight improvement of solvent quality, but further addition of CO_2 resulted in decreased solvent quality, as indicated by decreases in the dynamic second virial coefficients. These results demonstrate how the tunability of CO_2-expanded solutions can be used to increase polymer diffusion coefficients and to control solvent quality, which may be of practical use, particularly when working with catalytic polymer reaction systems.

Acknowledgements

The authors would like to thank Dr. John H. van Zanten of North Carolina State University for the helpful discussions. This research was supported by Contract W911NF-04-D-0003 from the United States Army Research Office, Research Triangle Park, NC. Partial support was also provided by the STC Program of the National Science Foundation under Agreement No. CHE-9876674. This material is also based upon work supported under a National Science Foundation Graduate Research Fellowship (LBD).

Appendix. Supplementary data

Supplementary data associated with this article can be found in the online version, at doi:10.1016/j.polymer.2009.09.069.

References

[1] Gehlsen M, Bates FS. Macromolecules 1993;26(16):4122–7.
[2] McManus NT, Rempel GL. Polym Rev 1995;35(2):239–85.
[3] Hahn SF. Hydrogenated polystyrene: preparation and properties. In: Scheirs J, Priddy DB, editors. Modern styrenic polymers: polystyrenes and styrenic copolymers. Hoboken, NJ: John Wiley and Sons; 2003. p. 533–55.
[4] Wei M, Musie GT, Busch DH, Subramaniam B. J Am Chem Soc 2002;124(11):2513–7.
[5] Kerler B, Robinson RE, Borovik AS, Subramaniam B. Appl Catal B 2004;49(2):91–8.
[6] Jin H, Subramaniam B, Ghosh A, Tunge J. AIChE J 2006;52(7):2575–81.
[7] Nakatani H, Nitta K, Soga K. Polymer 1998;39(18):4273–8.
[8] Zhao J, Hahn SF, Hucul DA, Meunier DM. Macromolecules 2001;34(6):1737–41.
[9] Ness JS, Brodil JC, Bates FS, Hahn SF, Hucul DA, Hillmyer MA. Macromolecules 2002;35(3):602–9.
[10] Xu D, Carbonell RG, Kiserow DJ, Roberts GW. Ind Eng Chem Res 2003;42(15):3509–15.
[11] Bussard A, Dooley KM. AIChE J 2008;54(4):1064–72.
[12] Xu D, Carbonell RG, Roberts GW, Kiserow DJ. J Supercrit Fluids 2005;34(1):1–9.
[13] Kermis TW, Li D, Guney-Altay O, Park I-H, van Zanten JH, McHugh MA. Macromolecules 2004;37(24):9123–31.
[14] Kostko AF, McHugh MA, van Zanten JH. Macromolecules 2006;39(4):1657–9.
[15] Guo J, Andre P, Adam M, Panyukov S, Rubinstein M, DeSimone JM. Macromolecules 2006;39(9):3427–34.
[16] Hammel GL, Schulz GV, Lechner MD. Makromol Chem 1981;182(6):1829–34.
[17] Michels A, Hamers J. Physica 1937;4(10):995–1006.
[18] Lemmon EW, McLinden MO, Friend DG. In: Linstrom PJ, Mallard WG, editors. NIST chemistry webbook: NIST standard reference database number 69. Gaithersburg, MD: National Institute of Standards and Technology; June 2005.
[19] DIPPR Data Ser; 1998.
[20] Cain NA, personal communication.
[21] Kotera A, Matsuda H, Konishi K, Takemura K. J Polym Sci Part C 1968;23(2):619–27.
[22] Yamakawa H. Modern theory of polymer solutions. New York: Harper & Row; 1971 [chapter 6].
[23] Tsunashima Y, Nemoto N, Kurata M. Macromolecules 1983;16(7):1184–8.
[24] Rubinstein M, Colby RH. Polymer physics. Oxford: Oxford University Press; 2003 [chapter 1].
[25] Nose T, Chu B. Macromolecules 1979;12(4):590–9.
[26] Okada R, Toyoshima Y, Fujita H. Makromol Chem 1963;59(1):137–49.
[27] Berry GC. J Chem Phys 1966;44(12):4550–64.
[28] Li D, Liu Z, Han B, Yang G, Wu Z, Liu Y, et al. Macromolecules 2000;33(21):7990–3.
[29] Jessop PG, Subramaniam B. Chem Rev 2007;107(6):2666–94.
[30] Tiffin DL, DeVera AL, Luks KD, Kohn JP. J Chem Eng Data 1978;23(1):45–7.
[31] Whittier RE, Xu D, van Zanten JH, Kiserow DJ, Roberts GW. J Appl Polym Sci 2006;99(2):540–9.
[32] Li D, Han B, Liu Z, Liu J, Zhang X, Wang S, et al. Macromolecules 2001;34(7):2195–201.